

Article

Convective and Microwave Assisted Drying of Wet Porous Materials with Prolate Spheroidal Shape: A Finite-Volume Approach

Edna G. Silva ¹, Ricardo S. Gomez ^{2,*}, Josivanda P. Gomes ³, Rossana M. F. Figueirêdo ³, Alexandre J. M. Queiroz ³, Wilton P. Silva ⁴, Ângela M. Santiago ⁵, Antonio D. B. Macedo ³, João P. L. Ferreira ³, Ítalo A. Gomes ⁶ and Antonio G. B. Lima ²

¹ Department of Physics, State University of Paraíba, Campina Grande 58429-500, Brazil; dinasansil@yahoo.com.br

² Department of Mechanical Engineering, Federal University of Campina Grande, Campina Grande 58429-900, Brazil; antonio.gilson@ufcg.edu.br

³ Department of Agricultural Engineering, Federal University of Campina Grande, Campina Grande 58429-900, Brazil; josivanda@gmail.com (J.P.G.); rossanamff@gmail.com (R.M.F.F.); alexandrejmq@gmail.com (A.J.M.Q.); daniel_buritt@hotmail.com (A.D.B.M.); joaop_l@hotmail.com (J.P.L.F.)

⁴ Department of Physics, Federal University of Campina Grande, Campina Grande 58429-900, Brazil; wiltonps@uol.com.br

⁵ Department of Chemical, State University of Paraíba, Campina Grande 58429-500, Brazil; angelamariasantiago01@gmail.com

⁶ Center of Exact and Applied Social Sciences, State University of Paraíba, Patos 58706-550, Brazil; italogomes.eng@gmail.com

* Correspondence: ricardosoaresgomez@gmail.com; Tel.: +55-83-98893-7991

Received: 10 October 2020; Accepted: 25 October 2020; Published: 28 October 2020



Abstract: Convective heating is a traditional method used for the drying of wet porous materials. Currently, microwave drying has been employed for this purpose, due to its excellent characteristics of uniform moisture removal and heating inside the material, higher drying rate, and low energy demand. This paper focuses on the study of the combined convective and microwave drying of porous solids with prolate spheroidal shape. An advanced mathematical modeling based on the diffusion theory (mass and energy conservation equations) written in prolate spheroidal coordinates was derived and the numerical solution using the finite-volume method is presented. Here, we evaluated the effect of the heat and mass transport coefficients and microwave power intensity on the moisture removal and heating of the solid. Results of the drying and heating kinetics and the moisture and temperature distribution inside the solid are presented and discussed. It was verified that the higher the convective heat and mass transfer coefficients and microwave power intensity, the faster the solid will dry and heat up.

Keywords: drying; microwave; convective; prolate spheroid; simulation

1. Introduction

Porous materials are a class of materials composed by a solid matrix with interconnected and disconnected pores of different shapes and sizes, and randomly distributed. In general, these void spaces are filled with one or more fluids. Several materials can be classified as porous materials such as fruits, vegetables and grains, which are rich in vitamins and minerals. Unfortunately, these post-harvested biological materials have high moisture content and are highly perishable.

Due to the great nutritional importance for human diet and nutrition, these materials must be dehydrated (moisture removal) in order to avoid nutritional, biological, physical or chemical

deterioration. In the present day, there are many dehydration techniques that can be used for this purpose, such as drying and osmotic dehydration. Drying is transient process that has occurred with several coupled phenomena, such as heat and mass transfer, phase change of the fluid (evaporation) inside the pores and dimension variations of the material related to moisture removal (shrinkage) and heating (dilation). The optimal idea is to apply this technique with minimum effect on the material from mechanical, biological, physical, chemical and energy saving points of view. Currently, there are various artificial drying techniques that include hot air (convective), freezing (freeze drying) and electromagnetic fields (solar, infrared, and microwave drying).

Since a microwave is a type of electromagnetic wave, it can be transmitted through the material, and reflected or absorbed by itself. The intensity of each of this effect is dependent on the material nature (dielectric properties) and the water content inside the material.

Microwave drying has been considered as an excellent method for dehydration of agricultural products, such as fruits, vegetables and grains, due to various advantages over other drying techniques, for example, convective and infrared drying, which include uniform moisture removal and heating, high drying rate, low energy demand and shorter drying time, resulting in an increased product quality [1–5]. Due to these excellent characteristics, microwave drying has been applied in many green agricultural products, such as grapes [5], bananas [6], mushrooms [7], pears [8], potatoes [9], tomatoes [10], and rough rice [11]. Many of these studies have devoted attention to experiments, mathematical modeling and simulations. Unfortunately, in the literature, most of these models are used in pre-established drying types and conditions are applied to each wet porous material treating it similar to a rectangular prism, plate, cylinder or sphere.

Based on the literature, it can be verified that some theoretical works have focused on the drying process of biological materials with non-conventional geometry, such as prolate spheroidal bodies—whole bananas [12–15]; wheat grain [16–20]; rice grain [21–26], and oblate spheroidal bodies—lentil grains [27–30]. According to these authors, the choice of an appropriate geometry for the materials enables better understanding of the drying process, more realistic moisture content and temperature distribution inside the materials, and the correct estimation of the mass diffusion coefficient and other process parameters, when compared with information considering material shapes such as spheres or cylinders. However, all these studies are related to convective drying only.

This way, there is a lack of opportunities for new research related to the microwave drying process for materials of non-conventional shapes, especially that applied to a hybrid drying process, for example, convective and microwave assisted drying.

In this sense, the aim of this work is to study combined microwave and convective drying of porous materials with a complex shape (prolate spheroidal body).

2. Methodology

2.1. The Geometry and Physical Problem

In this work, we consider a wet porous body with prolate spheroid shape heated by a hot fluid flowing around it and microwave power (Figure 1). Figure 2 illustrates some geometrical characteristics of this wet porous solid.

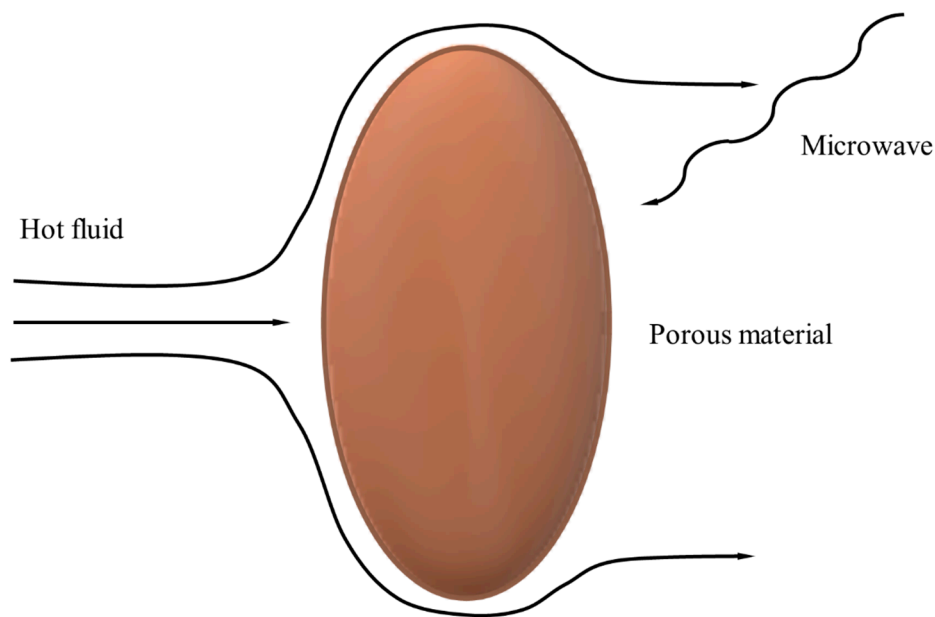


Figure 1. The physical problem studied in this work.

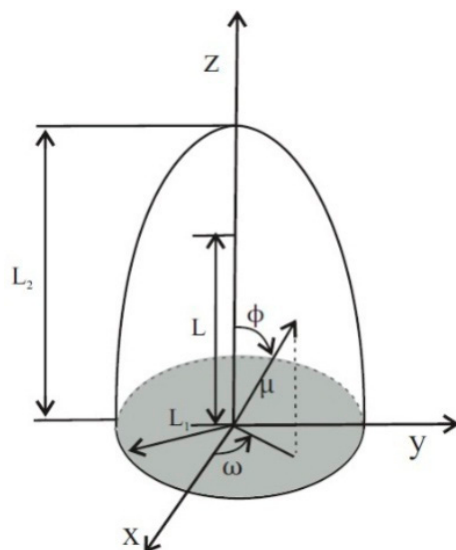


Figure 2. Geometrical parameters of a prolate spheroidal solid.

2.2. Mathematical Modeling

For an appropriate formulation, the following considerations are given:

- The porous body is assumed to be isotropic;
- The mass transport occurred only by diffusion inside the body and convection at the surface;
- The heat transfer occurred only by conduction and volumetric heating inside the solid, and convection at the surface;
- Thermo-physical properties are considered to be constant;
- Dimension variations were neglected.

Then, for mass transfer and based on the considerations cited earlier, Fick's second law of diffusion (two-dimensional case) was written in the prolate spheroidal coordinate system, as follows:

$$\frac{\partial M}{\partial t} = \left[\frac{1}{L^2(\xi^2 - \eta^2)} \frac{\partial}{\partial \xi} \left((\xi^2 - 1) D \frac{\partial M}{\partial \xi} \right) \right] + \left[\frac{1}{L^2(\xi^2 - \eta^2)} \frac{\partial}{\partial \eta} \left((1 - \eta^2) D \frac{\partial M}{\partial \eta} \right) \right] \quad (1)$$

where D is the mass diffusion coefficient and M the moisture content (dry basis).

For a well-posed formulation, the following initial and boundary conditions are used:

$$M = M_0 \text{ for } t = 0 \quad (2)$$

$$-D \nabla M|_s = h_m (M - M_e)|_s \text{ at the surface} \quad (3)$$

For heat transfer, we use the heat conduction equation (two-dimensional case) as follows:

$$\frac{\partial(\rho c_p T)}{\partial t} = \left[\frac{1}{L^2(\xi^2 - \eta^2)} \frac{\partial}{\partial \xi} \left((\xi^2 - 1) K_T \frac{\partial T}{\partial \xi} \right) \right] + \left[\frac{1}{L^2(\xi^2 - \eta^2)} \frac{\partial}{\partial \eta} \left((1 - \eta^2) K_T \frac{\partial T}{\partial \eta} \right) \right] + \dot{Q} \quad (4)$$

In this equation, ρ is the density of the dry solid, c_p is the specific heat, K_T is the thermal conductivity, T is the temperature and \dot{Q} is the volumetric heat generation.

For this governing equation, the initial and boundary conditions are as follows:

$$T = T_0 \text{ for } t = 0 \quad (5)$$

$$-K_T \nabla T|_s = h_c (T_{eq} - T)|_s \text{ at the surface} \quad (6)$$

For a better understanding, it can be stated the relationships between Cartesian and prolate spheroidal coordinate systems are follows [12]:

$$x = L \sqrt{(1 - \xi^2)(\eta^2 - 1)} \xi \quad (7)$$

$$y = L \sqrt{(1 - \xi^2)(\eta^2 - 1)} \sqrt{1 - \xi^2} \quad (8)$$

$$z = L \xi \eta \quad (9)$$

where $\xi = \cosh \mu$; $\eta = \cos \phi$; $\zeta = \cos \omega$ and $L = (L_2^2 - L_1^2)^{1/2}$ (Figure 2).

According to Lima et al. [4], an equation that has been reported in the literature for power absorbed and converted in heat during microwave irradiation can be expressed as:

$$\dot{Q} = P_0 \left(\frac{M(\vec{r}, t)}{M_0} \right) \varepsilon_r''(M, T) \exp(-2\Psi \vec{r} \cdot \vec{n}) \quad (10)$$

where P_0 is the power incident on the surface of the product (parameter to be determined experimentally), $M(\vec{r}, t)$ is the moisture content of the material, M_0 is the initial moisture content, \vec{r} is the position vector of the microwave within the material, \vec{n} is the unit vector normal to the surface, ε_r'' represents the dielectric loss factor relative to air and Ψ is the attenuation factor.

The depth of penetration (D_p) of the microwave and the attenuation factor are given by:

$$D_p = \frac{\lambda_0}{2\pi} \left[\varepsilon_r' \left(\sqrt{1 + \left(\frac{\varepsilon_r''}{\varepsilon_r'} \right)^2} - 1 \right)^{-1} \right]^{\frac{1}{2}} \quad (11)$$

$$\Psi = \frac{1}{D_p} \quad (12)$$

where ϵ'_r represents the dielectric constant of the material.

After obtaining the solution of Equations (1) and (4), the moisture content and temperature fields inside the material can be obtained throughout the process. Thus, the average moisture content and average temperature for the porous body during the drying process can be found using the following equations [31]:

$$\bar{M} = \frac{1}{V} \int_V M dV \quad (13)$$

$$\bar{T} = \frac{1}{V} \int_V T dV \quad (14)$$

2.3. Numerical Solution

To obtain the numerical solution of the heat and mass transfer equations (Equations (1) and (4)), the finite-volume method was used [32–34]. In this technique, the partial differential equation is integrated in volume and time. As a result, we obtain discretized linear algebraic equations for mass and heat transfer, as follows:

$$A_P \Phi_P = A_N \Phi_N + A_S \Phi_S + A_E \Phi_E + A_W \Phi_W + A_P^0 \Phi_P^0 + B \quad (15)$$

The coefficients A_K with $K \neq P$ represent the contributions of the diffusive transport of the variable Φ coming from the neighboring nodal points in the direction of node P . The coefficient A_P^0 reflects the influence of the variable Φ in the previous time on its value in the present time. For mass transfer, we have $\Phi = M$ and $B = 0$, while for heat transfer, we have $\Phi = T$ and $B = \dot{Q} \neq 0$.

To obtain the simulated results, a computational code was implemented in the Mathematica® software, using a uniform mesh with 20×20 nodal points (Figure 3) and time step $\Delta t = 1.0$ s, each obtained after refining the grid and time step. For the solution of the set of algebraic linear equations (Equation (15)), we used the Gauss–Seidel interactive method with a convergence criterion of 10^{-8} kg/kg for moisture content and 10^{-8} K for temperature.

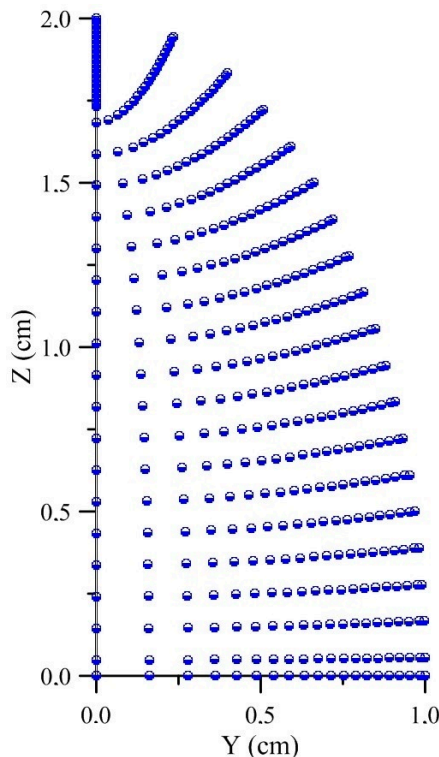


Figure 3. The numerical grid in the physical domain used in the simulations.

2.4. Validation

For validation of the proposed model, two different cases were considered:

- (a) Mass transfer process in a prolate spheroidal body $\dot{Q} = 0$, without heat transfer and convective condition at the surface.

For this particular case, the following data were used: $L_1 = 1.000 \text{ cm}$, $L_2 = 2.000 \text{ cm}$, $Bi_m = 1.0$, $D = 1.220 \times 10^{-9} \text{ m}^2/\text{s}$, $M_0 = 5.432 \text{ kg/kg}$ (dry basis), $M_e = 0.084 \text{ kg/kg}$ (dry basis), $T_0 = 5.432 \text{ K}$ and $T_e = 0.084 \text{ K}$.

- (b) Heating process of a spherical body with a constant volumetric heat source, without mass transfer and equilibrium condition at the surface.

Here, the following data were used: $L_1 = 1.000 \text{ cm}$ and $L_2 = 1.001 \text{ cm}$; $P_0 = 10^6 \text{ W/m}^3$; $\Psi = 0.0 \text{ m}^{-1}$; $c_p = 3395 \text{ J/kgK}$; $K_T = 0.3395 \text{ W/mK}$; $T_0 = 10^{-15} \text{ K}$; $T_e = 0.0 \text{ K}$; $h_c = 10^{30} \text{ W/m}^2\text{K}$; $\alpha = (K_T / \rho c_p) = 10^{-7} \text{ m}^2/\text{s}$ and $\rho = 1000 \text{ kg/m}^3$, and the radius of the sphere $R = L_1$.

According to Carslaw and Jaeger [35], the analytical solution of the appropriated energy equation has the following form:

$$g(r, t) = \left(-\frac{2R}{\pi^2 r K_T} \right) \sum_{n=1}^{\infty} \frac{1}{n^2} \left[\sin\left(\frac{n\pi r}{R}\right) \int_0^R r' \sin\left(\frac{n\pi r'}{R}\right) f(r') dr' \right] \exp\left(-\frac{\alpha n^2 \pi^2 t}{R^2}\right) + \frac{1}{K_T} \left[\frac{1}{r} \int_0^r r'^2 f(r') dr' + \int_r^R r' f(r') dr' - \frac{1}{R} \int_0^R r'^2 f(r') dr' \right] \quad (16)$$

where,

$$\dot{Q} = f(r') = P_0 \quad (17)$$

2.5. Simulated Cases

Microwave drying and heating simulations were performed for one prolate spheroid with aspect ratio $L_2/L_1 = 2.0$, considering constant thermo-physical properties given in terms of the dimensionless parameters, mass and heat transfer Biot numbers ($Bi_m = h_m L_1 / D$ and $Bi_c = h_c L_1 / K_T$), mass transfer Fourier number ($Fo_m = Dt / L_1^2$) and the heat generation source term (\dot{Q}).

Table 1 presents a summary of the simulated cases. The following arbitrary data were considered in this research: initial moisture content ($M_0 = 0.20 \text{ kg/kg}$ dry basis), initial temperature ($T_0 = 298.16 \text{ K}$), drying-air temperature ($T_{eq} = 373.16 \text{ K}$), mass diffusion coefficient ($D = 1.22 \times 10^{-9} \text{ m}^2/\text{s}$), specific heat ($c_p = 3395 \text{ J/kg}\cdot\text{K}$), density ($\rho = 1000 \text{ kg/m}^3$) and thermal conductivity ($K_T = 0.3395 \text{ W/m}\cdot\text{K}$).

Table 1. Parameters used in the simulations for the microwave drying and heating.

Case	$L_2/L_1 (-)$	$h_m (\text{m/s})$	$h_c (\text{W/m}^2\text{K})$	$P_0 (\text{W/m}^3)$	$Bi (-)$	$\Psi (\text{m}^{-1})$
1	2.000	1.22×10^{-7}	33.95	1.0×10^3	1.0	0.0
2	2.000	3.66×10^{-7}	101.85	1.0×10^3	3.0	0.0
3	2.000	6.10×10^{-7}	169.75	1.0×10^3	5.0	0.0
4	2.000	12.20×10^{-7}	339.50	1.0×10^3	10.0	0.0
5	2.000	1.00×10^{30}	1.00×10^{30}	1.0×10^3	∞	0.0
6	2.000	6.10×10^{-7}	169.75	1.0×10^7	5.0	0.0
7	2.000	6.10×10^{-7}	169.75	1.0×10^6	5.0	0.0
8	2.000	6.10×10^{-7}	169.75	1.0×10^5	5.0	0.0
9	2.000	6.10×10^{-7}	169.75	1.0×10^4	5.0	0.0
10	2.000	6.10×10^{-7}	169.75	1.0×10^6	5.0	0.0
11	2.000	6.10×10^{-7}	169.75	1.0×10^6	5.0	1.0
12	2.000	6.10×10^{-7}	169.75	1.0×10^6	5.0	10.0
13	2.000	6.10×10^{-7}	169.75	1.0×10^6	5.0	50.0
14	2.000	6.10×10^{-7}	169.75	1.0×10^6	5.0	100.0

3. Results

Figure 4 illustrates a comparison between the predicted moisture ratio $\overline{M}^* = (M - M_e) / (M_0 - M_e)$ in a prolate spheroidal solid with the analytical results reported in the literature by [36–38]. The results are purely related to the convective drying phenomenon. From the analysis of this figure, it can be seen that there is an excellent concordance between the results. Thus, validating the model and methodology presented herein.

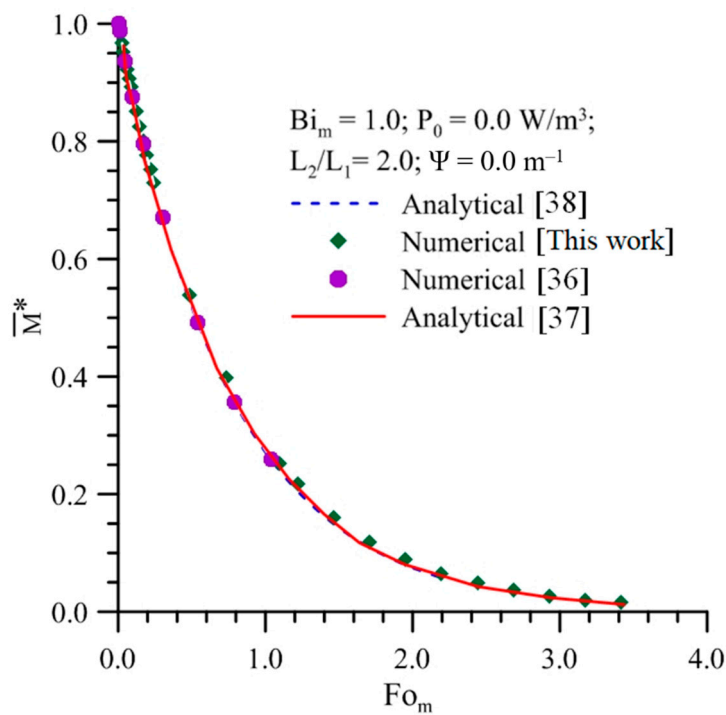


Figure 4. Comparison between the predicted and analytical moisture ratio as a function of the time for convective drying of a prolate spheroidal solid.

Figure 5 illustrates a comparison between the predicted and analytical results of the dimensionless parameter $[6 K_T (T - T_0) / (P_0 L_1^2)]$ [35] within a sphere of radius $L_1 = 1.0$ cm for different Fourier numbers ($Fo_c = \alpha t / L_1^2 = 0.06, 0.10, 0.20$ and 0.60). This physical problem corresponds to an intense heat convection condition at the surface of the sphere in conjunction with an intense microwave heating with constant heating power density $P_0 = 10^6$ W/m³, and considering the attenuation factor $\Psi = 0.0$ m⁻¹. Again, from the analysis of this figure, it can be seen that there is an excellent concordance between the results.

Figures 6 and 7 (cases one to five of Table 1) present the average moisture content and average temperature in a prolate spheroidal solid with aspect ratio $L_2/L_1 = 2.0$ for different mass transfer Biot numbers ($Bi_m = Bi_c$). In these figures, $Bi_c = 1.0$ corresponds to a weak heat convection phenomenon at the surface of the solid and $Bi_c \rightarrow \infty$ corresponds to a strong physical interaction of the thermal convection, i.e., instantaneously the surface temperature equals the temperature of the drying-air and the moisture content at the surface reaches its hygroscopic equilibrium condition. From the analyses of these figures, it is observed that an increase in the Biot number (mass or heat) provides an increase in the drying and heating rates of the solid, that is, the body reaches hygroscopic and thermal equilibrium in a shorter process time. A small value of mass transfer Biot number causes a decrease in the drying rate of the material and therefore a longer exposure time to the microwave radiation, which can cause damage to the product being dried. Meanwhile, with a higher heat transfer Biot number, the material

reaches the thermal equilibrium in a shorter heating time. Further, it can be stated that the heating process of the solid is faster than the drying process.

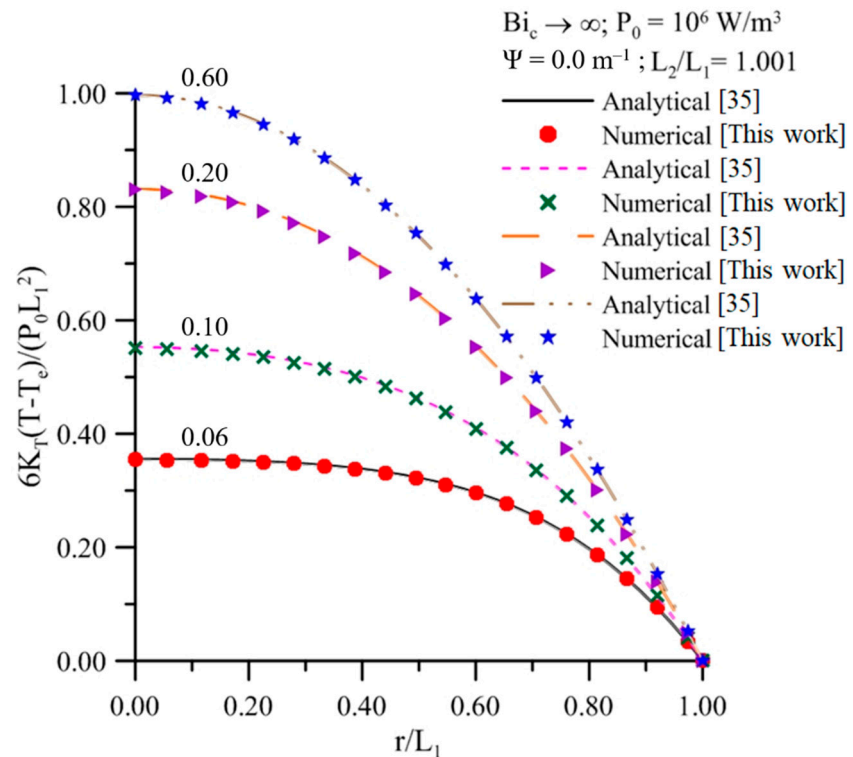


Figure 5. Dimensionless temperature behavior in a sphere with zero surface temperature and constant heat production for different heat transfer Fourier numbers.

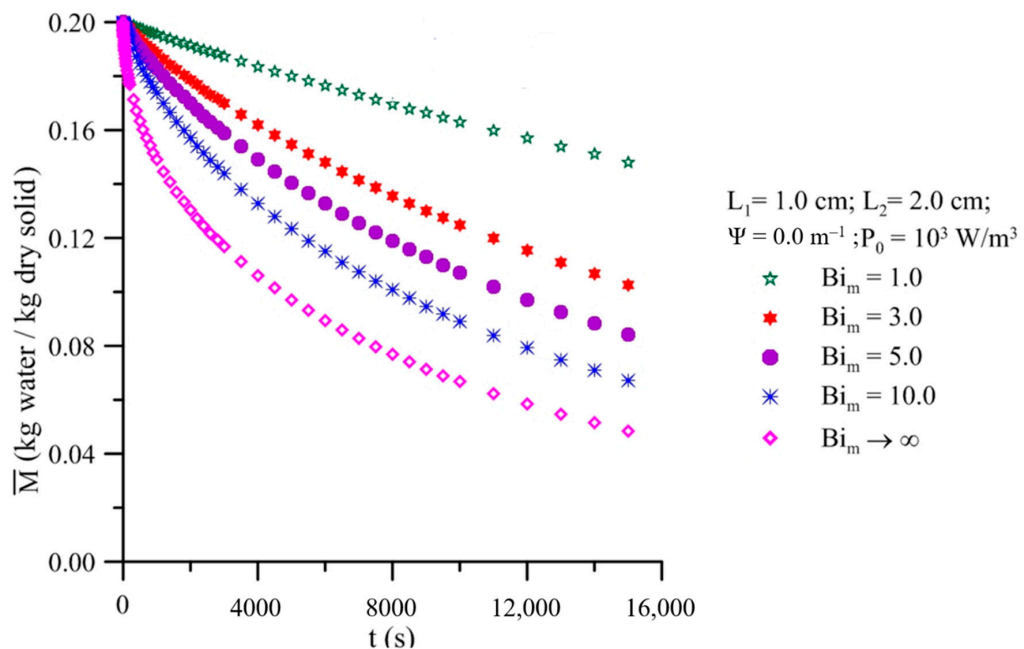


Figure 6. Transient behavior of the average moisture content in a prolate spheroidal solid with aspect ratio 2.0, different mass transfer Biot numbers and fixed microwave power density.

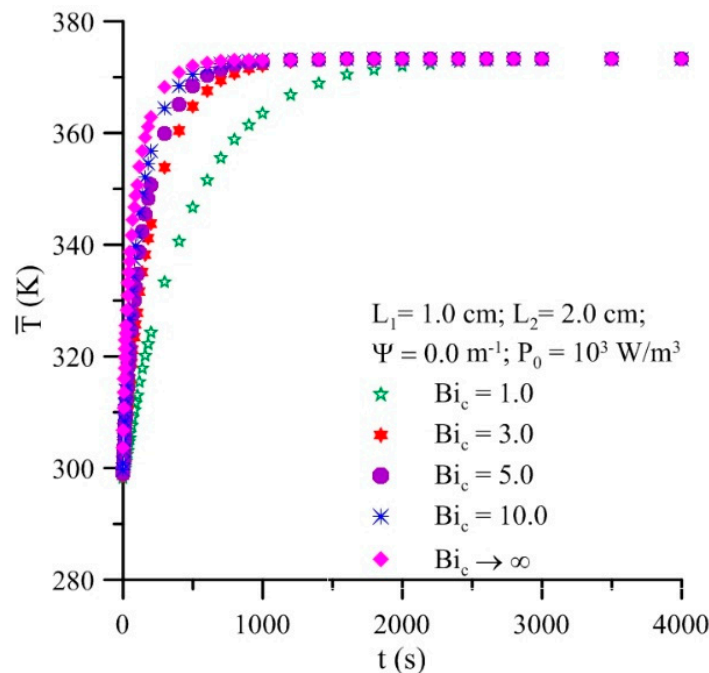


Figure 7. Transient behavior of the average temperature in a prolate spheroidal solid with aspect ratio 2.0, different heat transfer Biot numbers and fixed microwave power density.

Figures 8 and 9 (cases one to five of Table 1) present the moisture content profiles on the y -axis ($z = 0$) inside a prolate spheroidal solid with aspect ratio $L_2/L_1 = 2.0$ for different mass transfer Biot numbers at different moments of drying. Analyzing these figures, it is verified that an increase in the Biot number (mass) corresponds to an increase in the drying rate, which leads to higher moisture gradients inside the solid, especially in the initial drying moments and near the surface of the solid.

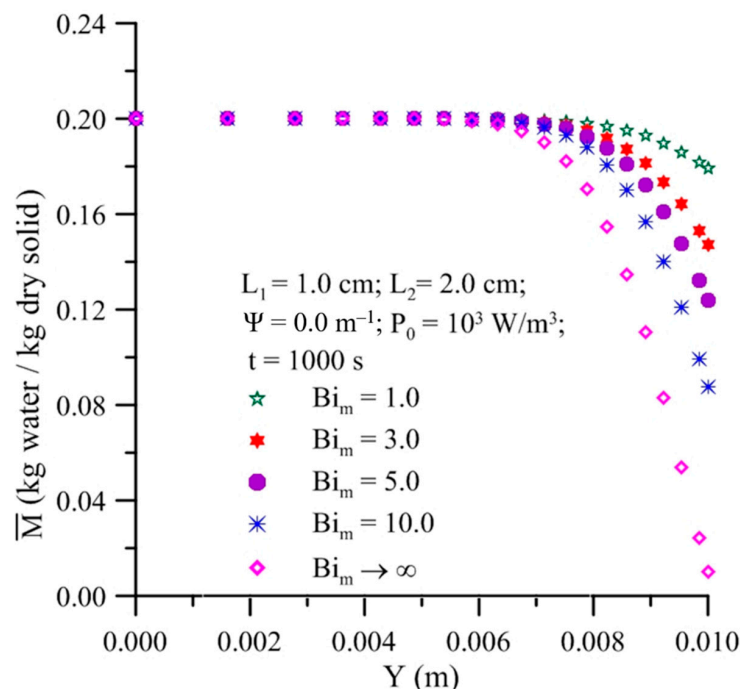


Figure 8. Moisture content inside a prolate spheroidal solid with aspect ratio $L_2/L_1 = 2.0$, different mass transfer Biot numbers and fixed microwave power density (y -axis, $z = 0$, $t = 1000 \text{ s}$).

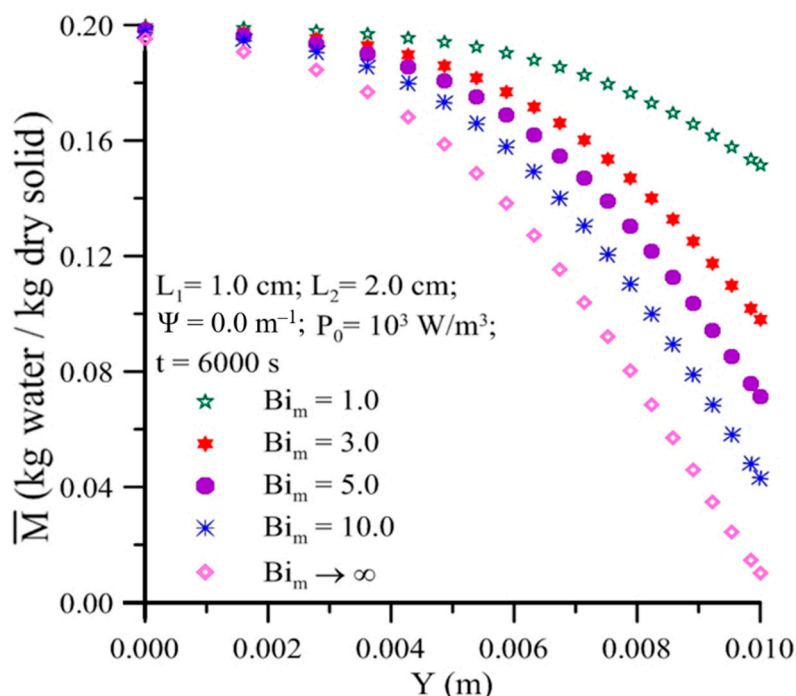


Figure 9. Moisture content inside a prolate spheroidal solid with aspect ratio $L_2/L_1 = 2.0$, different mass transfer Biot numbers and fixed microwave power density (y -axis, $z = 0$, $t = 6000 \text{ s}$).

Figures 10–12 (cases one to five of Table 1) show the temperature profiles on the y -axis ($z = 0$) for a prolate spheroidal solid with aspect ratio 2.0 and different heat transfer Biot numbers at the instants of time 300, 1000 and 4000 s, respectively. By analyzing these figures, it is noticed that an increase in the heat transfer Biot number implies a higher heating rate of the solid, thus reaching its equilibrium temperature at the surface more quickly. In the initial heating times, the heat flux occurs from the surface to the center of the solid, i.e., the heating process is governed by heat convection. After a certain warm-up period, this behavior is reversed, and heat flux occurs from the center to the surface of the solid. Now, the heating process is governed by microwave heating, and the lower the heat transfer Biot number, the higher the temperature inside the prolate spheroidal solid, for a longer drying time. From the physical point of view, when the value of the heat transfer Biot number is small, one has a physical situation with low heat transfer by convection and the microwave heating dominates the phenomenon.

Figures 13 and 14 (cases six to nine of Table 1) illustrate the temperature distribution within a prolate spheroidal solid with aspect ratio $L_2/L_1 = 2.0$ for different microwave power densities and different moments of the drying process. By analyzing these figures, it can be observed that for the microwave power densities ranging from 10^4 to 10^6 W/m^3 , the temperature profiles showed similar behaviors; however, for the higher microwave power density of 10^7 W/m^3 , there was a substantial increase in temperature at the beginning of the microwave heating process, which may cause damage to the physical structure of the product being heated or even fully incinerated. Furthermore, it is known that the higher the applied microwave power density, the greater the amount of heat generated internally in the product, providing greater rigidity and less shrinkage. Obviously, these phenomena are dependent on the nature of the product, for example, biological and non-biological materials, especially for heat sensitive materials such as fruit, vegetables, grains, and many others.

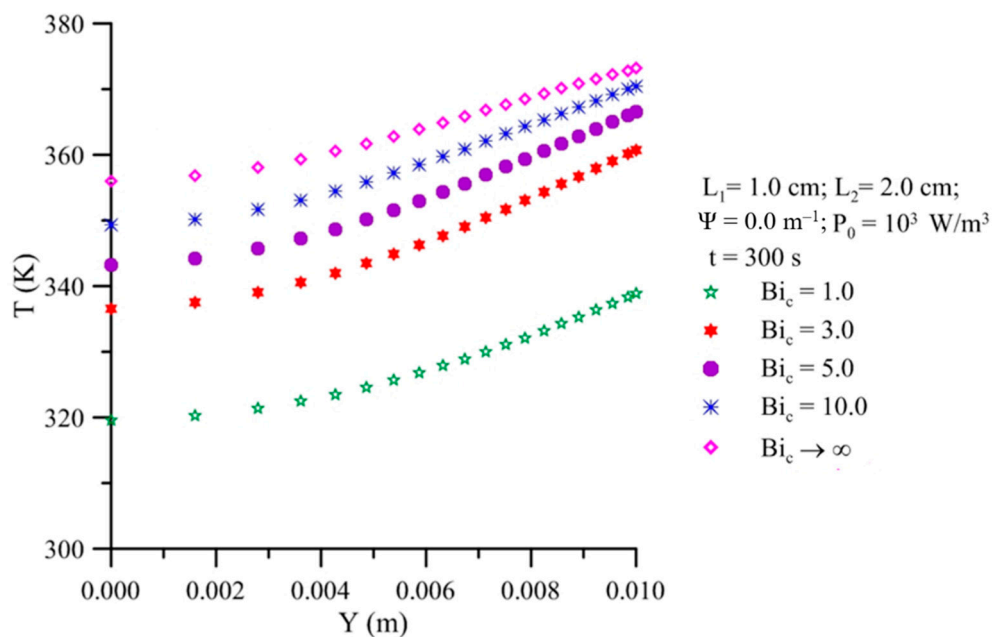


Figure 10. Temperature inside a prolate spheroidal solid with aspect ratio $L_2/L_1 = 2.0$, different heat transfer Biot numbers and fixed microwave power density (y -axis, $z = 0$, $t = 300 \text{ s}$).

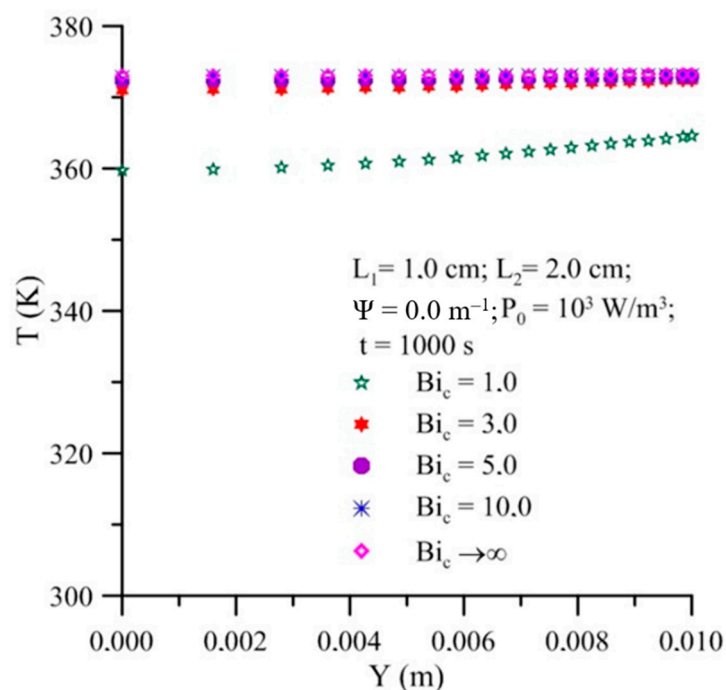


Figure 11. Temperature inside a prolate spheroidal solid with aspect ratio $L_2/L_1 = 2.0$, different heat transfer Biot numbers and fixed microwave power density (y -axis, $z = 0$, $t = 1000 \text{ s}$).

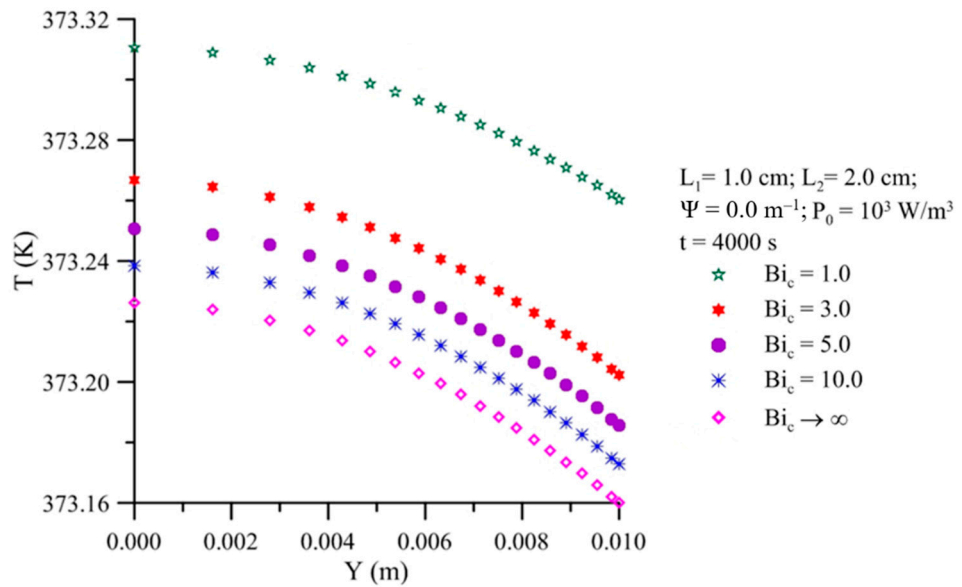


Figure 12. Temperature inside a prolate spheroidal solid with aspect ratio $L_2/L_1 = 2.0$, different heat transfer Biot numbers and fixed microwave power density (y -axis, $z = 0$, $t = 4000 \text{ s}$).

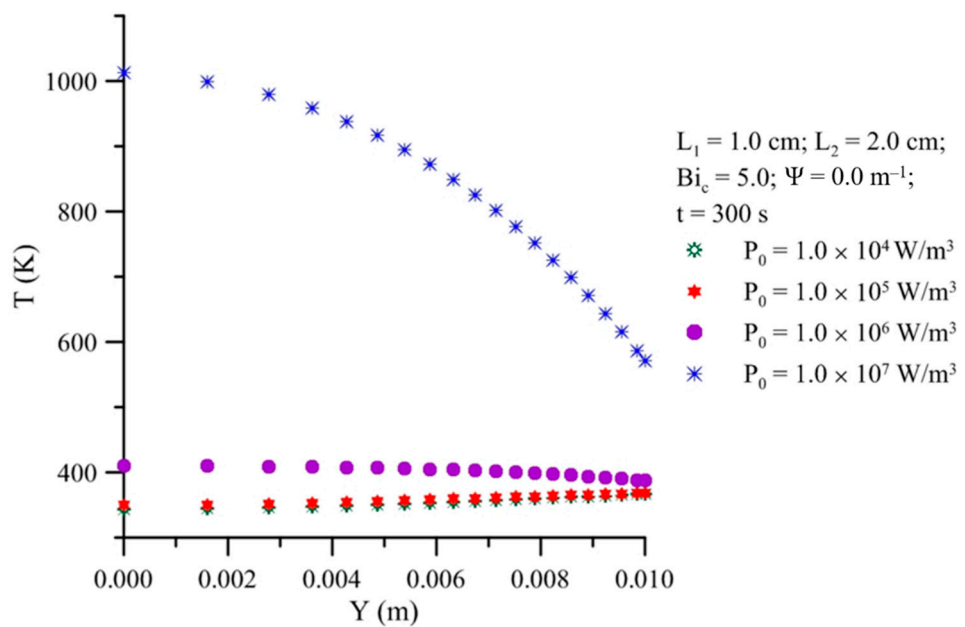


Figure 13. Temperature inside a prolate spheroidal solid with aspect ratio $L_2/L_1 = 2.0$, different microwave power densities and fixed heat transfer Biot number (y -axis, $z = 0$, $t = 300 \text{ s}$).

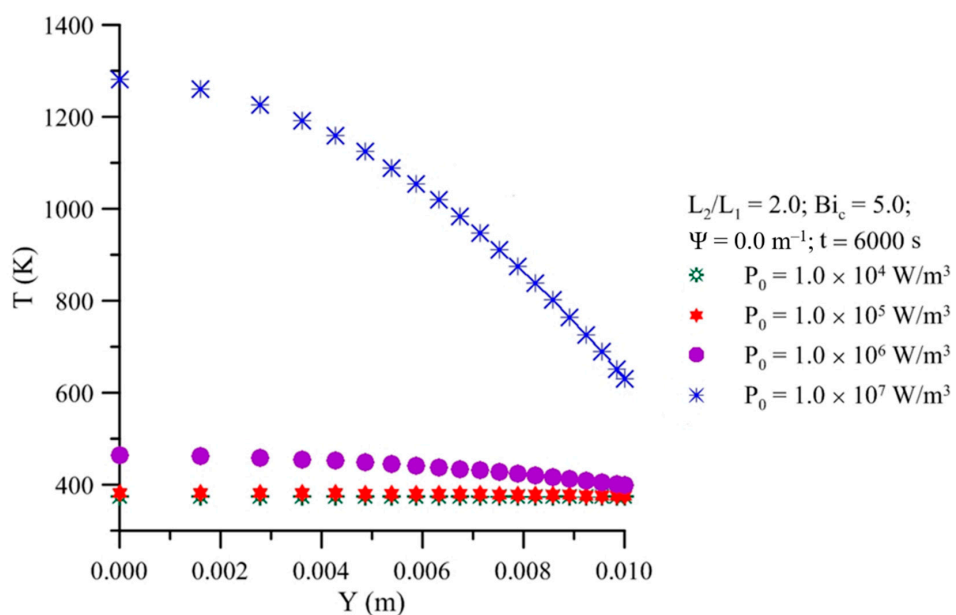


Figure 14. Temperature inside a prolate spheroidal solid with aspect ratio $L_2/L_1 = 2.0$, different microwave power densities and fixed heat transfer Biot number (y -axis, $z = 0$, $t = 6000 \text{ s}$).

Figure 15 (cases 10 to 14 of Table 1) illustrates the heating kinetics of a prolate spheroidal solid for different attenuation factors of the electromagnetic waves when subjected to a microwave power density of 10^6 W/m^3 and heat transfer Biot number equal to 5.0. Upon analyzing this figure, it can be seen that the temperature increases with time, and this phenomenon is more intense for lower attenuation factors. For this physical situation, we have a greater depth of penetration of the electromagnetic waves, providing faster heating or even incineration of the porous body.

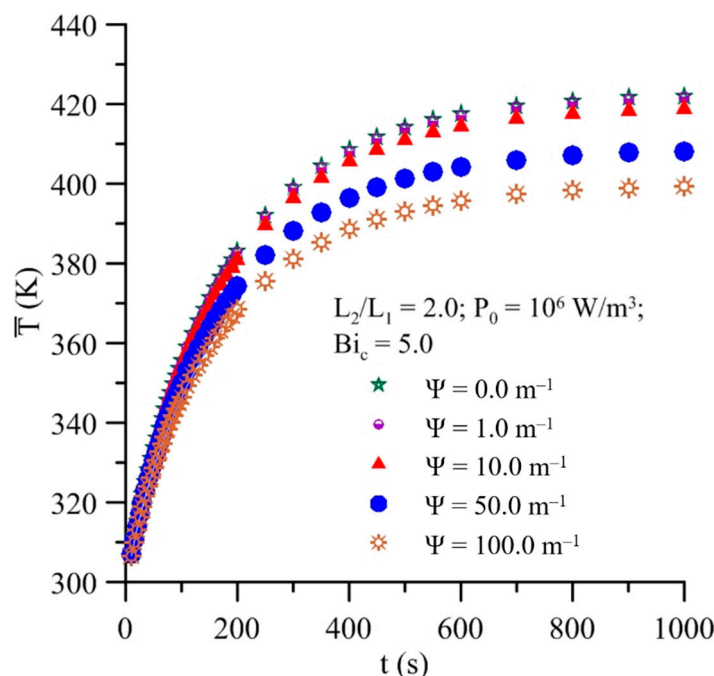


Figure 15. Transient behavior of the average temperature inside a prolate spheroidal solid with aspect ratio $L_2/L_1 = 2.0$ for different attenuation factors and fixed microwave power density and heat transfer Biot number.

Figure 16 (cases 10 to 14 of Table 1) illustrates the temperature distribution inside a prolate spheroidal solid with aspect ratio $L_2/L_1 = 2.0$ for different attenuation factors and fixed microwave power density and heat transfer Biot number at 900 s. By analyzing the temperature profile on the y -axis ($z = 0$), it is observed that the highest temperature value, 461.28 K, occurred just for the lowest attenuation factor ($\Psi = 0.0 \text{ m}^{-1}$). This is due to the fact that the attenuation factor is inversely proportional to the penetration depth of the electromagnetic waves, which is mainly responsible for the rise in temperature during the microwave heating process for wet solids. The high temperature value inside the product can cause irreparable damage to the product and may even incinerate it.

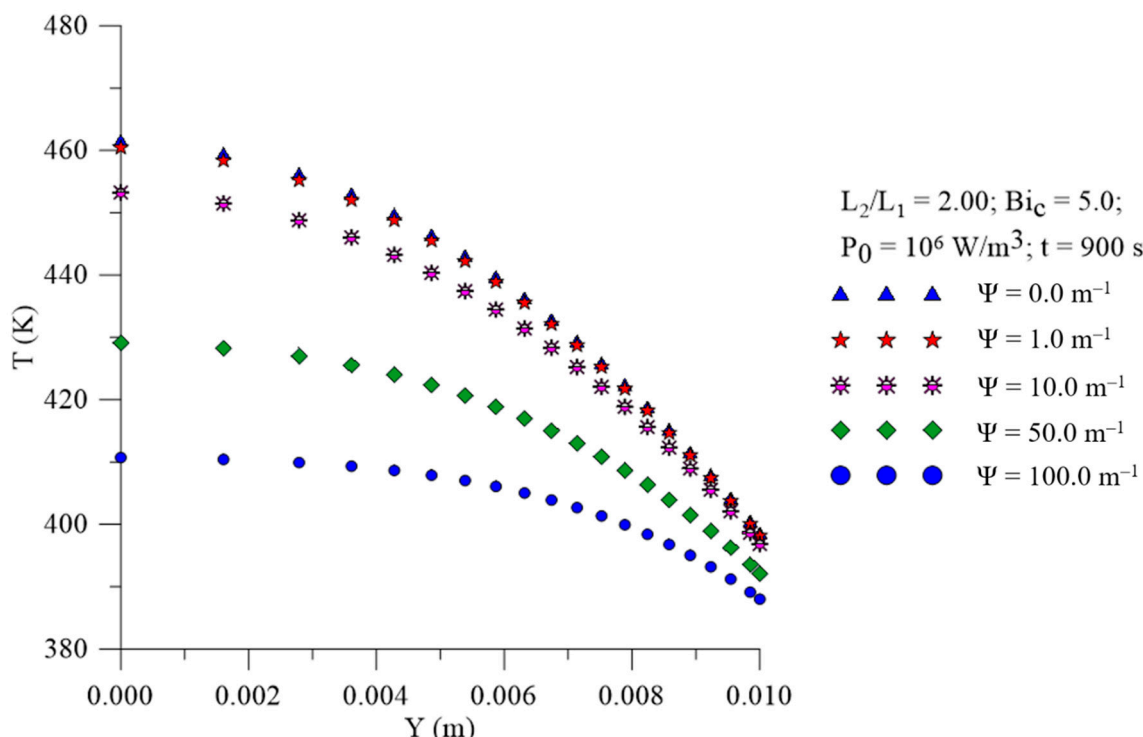


Figure 16. Temperature inside a prolate spheroidal solid with aspect ratio $L_2/L_1 = 2.0$, different attenuation factors and fixed microwave power density and heat transfer Biot number (y -axis, $z = 0$, $t = 900$ s).

4. Conclusions

In this paper, an advanced study to predict coupled microwave heating and drying processes of a wet porous material with complex geometric shape (ranging from sphere and prolate spheroid to infinite cylinder) was developed. All formalism of the mathematical model and numerical solution of the governing equations were presented. From the obtained results, it can be concluded that:

- (a) For a fixed microwave power density, a drying process with a higher Biot number for heat and mass transfer will result in the solid drying and heating up faster. The effect is more evident in moisture ratio than in average temperature;
- (b) In hybrid processes, for a shorter drying time, moisture migration occurs from the center to the surface and heat flux occurs in the opposite direction, generating high thermal and hydric gradients inside the solid;
- (c) In hybrid processes, for a longer dying time, moisture migration and heat flux occurs in the same direction, from the center to the surface, generating low hydric gradients and high thermal gradients inside the solid;

- (d) The higher the microwave power density, the greater the amount of heat generated, and the higher the temperature inside the solid. For the drying of prolate spheroidal solids, a microwave power density less than 10^6 W/m^3 provoked temperatures less than 450 K inside the solid.
- (e) The lower the attenuation factor (higher penetration depth), the higher the temperature inside the solid. For the drying of prolate spheroidal solids, an attenuation factor less than 50 m^{-1} provoked an average temperature greater than 410 K inside the solid.

Author Contributions: Conceptualization, E.G.S., J.P.G., R.M.F.F., A.J.M.Q., W.P.S., J.P.L.F., Í.A.G. and A.G.B.L.; Formal analysis, J.P.G., R.M.F.F., A.J.M.Q., W.P.S., A.D.B.M., J.P.L.F. and Í.A.G.; Investigation, E.G.S., R.S.G., J.P.G., Â.M.S. and Í.A.G.; Methodology, E.G.S., J.P.G., A.J.M.Q., Â.M.S., A.D.B.M., J.P.L.F. and Í.A.G.; Software, E.G.S., R.S.G., A.J.M.Q., W.P.S., Â.M.S., A.D.B.M., J.P.L.F. and A.G.B.L.; Supervision, R.M.F.F., W.P.S., Â.M.S. and A.G.B.L.; Validation, R.M.F.F., A.D.B.M. and A.G.B.L.; Visualization, R.S.G.; Writing—original draft, E.G.S., A.J.M.Q. and W.P.S.; Writing—review & editing, R.S.G., R.M.F.F., Â.M.S. and A.G.B.L. All authors have read and agreed to the published version of the manuscript.

Funding: This research was funded by CNPq, CAPES, FINEP (Brazilian research agencies).

Acknowledgments: The authors are grateful to the Federal University of Campina Grande (Brazil) and the State University of Paraíba (Brazil) for the research infrastructure and the references cited in the manuscript.

Conflicts of Interest: The authors declare no conflict of interest.

References

1. Haghi, A.K.; Amanifard, N. Analysis of heat and mass transfer during microwave drying of food products. *Braz. J. Chem. Eng.* **2008**, *25*, 491–501. [[CrossRef](#)]
2. Dunaeva, T.; Manturov, A. The phenomenological model microwave drying kinetics of food products. In Proceedings of the International Kharkov Symposium on Physics and Engineering of Microwaves, Millimeter and Submillimeter Waves (MSMW), Kharkov, Ukraine, 21–26 June 2004; pp. 1–3. [[CrossRef](#)]
3. Metaxas, A.C.; Meredith, R.J. *Industrial Microwave Heating*; Peter Peregrinus Ltd.: London, UK, 1983.
4. Lima, A.G.B.; Delgado, J.M.P.Q.; Silva, E.G.; Farias Neto, S.R.; Santos, J.P.S.; Lima, W.M.P.B. Drying process in electromagnetic fields. In *Drying and Energy Technologies*; Delgado, J.M.P.Q., Lima, A.G.B., Eds.; Springer International Publishing: Cham, Switzerland, 2016; pp. 89–110.
5. Bingo, L.G.; Pan, Z.; Roberts, J.S.; Devres, Y.O.; Balaban, M.O. Mathematical modeling of microwave-assisted convective heating and drying of grapes. *Int. J. Agric. Biol. Eng.* **2008**, *1*, 46–54. [[CrossRef](#)]
6. Maskan, M. Microwave/air and microwave finish drying of banana. *J. Food Eng.* **2000**, *44*, 71–78. [[CrossRef](#)]
7. Torringa, E.; Esveled, E.; Scheewe, I.; Bartels, P.; Berg, R. Osmotic dehydration as a pre-treatment before combined microwave-hot-air drying of mushrooms. *J. Food Eng.* **2001**, *49*, 185–191. [[CrossRef](#)]
8. Fumagalli, F. Pear Drying in Microwave Drier. Master’s Thesis, Federal University of São Carlos, São Carlos, Brazil, 2003. (In Portuguese)
9. Srikiatden, J.; Roberts, J.S. Measuring moisture diffusivity of potato and carrot (core and cortex) during convective hot air and isothermal drying. *J. Food Eng.* **2006**, *74*, 143–152. [[CrossRef](#)]
10. Ribeiro, R.C. Semi-Dehydrated Tomatoes Obtained by Drying Convective Microwaves Preceded by Osmotic Dehydration. Master’s Thesis, Federal University of Lavras, Lavras, Brazil, 2013. (In Portuguese)
11. Silva, E.G. Combined (Convective and Microwave) Drying of Prolate Spheroidal Solids: Modeling, Simulation and Experimentation. Ph.D. Thesis, Federal University of Campina Grande, Campina Grande, Brazil, 2016. (In Portuguese)
12. Lima, A.G.B.; Queiroz, M.R.; Nebra, S.A. Simultaneous moisture transport and shrinkage during drying of solids with ellipsoidal configuration. *Chem. Eng. J.* **2002**, *86*, 85–93. [[CrossRef](#)]
13. Lima, A.G.B.; Queiroz, M.R.; Nebra, S.A. Heat and mass transfer model including shrinkage applied to ellipsoidal products: Case study for drying of bananas. *Dev. Chem. Eng. Miner. Process.* **2002**, *10*, 281–304. [[CrossRef](#)]
14. Lima, A.G.B.; Farias Neto, S.R.; Silva, W.P. Heat and mass Transfer in Porous Materials with Complex Geometry: Fundamentals and Applications. In *Heat and Mass Transfer in Porous Media*, 1st ed.; Series: Advanced Structured Materials; Springer: Heidelberg, Germany, 2011; Volume 13, pp. 161–185. [[CrossRef](#)]

15. Lima, A.G.B.; Farias, R.P.; Silva, W.P.; Farias Neto, S.R.; Farias, F.P.M.; Lima, W.M.P.B. *Convective Drying of Food: Foundation, Modeling and Applications In Advanced Structured Materials*, 1st ed.; Springer International Publishing: Heidelberg, Germany, 2014; Volume 48, pp. 95–115. [[CrossRef](#)]
16. Oliveira, V.A.B.; Lima, A.G.B. Drying of wheat based on the non-equilibrium thermodynamics: A numerical study. *Dry. Tech.* **2009**, *27*, 306–313. [[CrossRef](#)]
17. Oliveira, V.A.B.; Lima, W.C.P.B.; Farias Neto, S.R.; Lima, A.G.B. Heat and mass diffusion and shrinkage in prolate spheroidal bodies based on non-equilibrium thermodynamics: A numerical investigation. *J. Porous Media* **2011**, *14*, 593–605. [[CrossRef](#)]
18. Lima, A.G.B.; Delgado, J.M.P.Q.; Oliveira, V.A.B.; Melo, J.C.S.; Joaquina e Silva, C. Porous Materials Drying Model Based on the Thermodynamics of Irreversible Processes: Background and Application. In *Advanced Structured Materials*, 1st ed.; Springer International Publishing: Heidelberg, Germany, 2014; Volume 48, pp. 1–23. [[CrossRef](#)]
19. Lima, A.G.B.; Delgado, J.M.P.Q.; Santos, I.B.; Silva Santos, J.P.; Barbosa, E.S.; Joaquina e Silva, C. GBI Method: A Powerful Technique to Study Drying of Complex Shape Solids. In *Advanced Structured Materials*, 1st ed.; Springer International Publishing: Heidelberg, Germany, 2014; Volume 48, pp. 25–43. [[CrossRef](#)]
20. Santos, J.P.S.; Santos, I.B.; Pereira, E.M.A.; Silva, J.V.; Lima, A.G.B. Wheat Convective Drying: An Analytical Investigation via Galerkin-Based Integral Method. *Def. Diffus. Forum* **2015**, *365*, 82–87. [[CrossRef](#)]
21. Hacihaftizoğlu, O.; Cihan, A.; Kahveci, K.; Lima, A.G.B. A liquid diffusion model for thin-layer drying of rough rice. *Eur. Food Res. Technol.* **2008**, *226*, 787–793. [[CrossRef](#)]
22. Cihan, A.; Kahveci, K.; Hacihaftizoğlu, O.; Lima, A.G.B. A diffusion based model for intermittent drying of rough rice. *Heat Mass Transf.* **2008**, *44*, 905–911. [[CrossRef](#)]
23. Silva, J.V.; Silva, F.N.; Andrade, T.H.F.; Lima, A.G.B. Drying of Rough Rice: A Numerical Investigation. *Defect Diffus. Forum* **2013**, *334–335*, 131–136. [[CrossRef](#)]
24. Franco, C.M.R.; Lima, A.G.B.; Silva, J.V.; Nunes, A.G. Applying Liquid Diffusion Model for Continuous Drying of Rough Rice in Fixed Bed. *Defect Diffus. Forum* **2016**, *369*, 152–156. [[CrossRef](#)]
25. Franco, C.M.R.; de Lima, A.G.B.; Farias, V.S.O.; Silva, W.P. Modeling and experimentation of continuous and intermittent drying of rough rice grains. *Heat Mass Transf.* **2020**, *56*, 1003–1014. [[CrossRef](#)]
26. Franco, C.M.R.; Lima, A.G.B.; Farias, V.S.O.; Machado, E.A. Intermittent Drying of Rice Grains with Husk: Modelling and Experimentation. *Diffus. Found.* **2020**, *25*, 9–36. [[CrossRef](#)]
27. Carmo, J.E.F.; Lima, A.G.B. Drying of Lentil Including Shrinkage: A Numerical Simulation. *Drying Technol.* **2005**, *23*, 1977–1992. [[CrossRef](#)]
28. Carmo, J.E.F.; de Lima, A.G.B.; Silva, C.J. Continuous and Intermittent Drying (Tempering) of Oblate Spheroidal Bodies: Modeling and Simulation. *Int. J. Food Eng.* **2012**, *8*. [[CrossRef](#)]
29. Melo, J.C.S.; Lima, A.G.B.; Silva, W.P.; Lima, W.M.P.B. Heat and Mass Transfer during Drying of Lentil Based on the Non-Equilibrium Thermodynamics: A Numerical Study. *Defect Diffus. Forum* **2015**, *365*, 285–290. [[CrossRef](#)]
30. Melo, J.C.S.; Gomez, R.S.; Silva Júnior, J.B.; Queiroga, A.X.M.; Dantas, R.L.; Lima, A.G.B.; Silva, W.P. Drying of Oblate Spheroidal Solids via Model Based on the Non-Equilibrium Thermodynamics. *Diffus. Found.* **2020**, *25*, 83–98. [[CrossRef](#)]
31. Whitaker, S. Heat and mass transfer in granular porous media. In *Advances in Drying*; Mujumdar, A.S., Ed.; Hemisphere Publishing Company: London, UK, 1980; Volume 1, pp. 23–61.
32. Patankar, S. *Numerical Heat Transfer and Fluid Flow*; CRC Press: Boca Raton, FL, USA, 1980.
33. Versteeg, H.K.; Malalasekera, W. *An Introduction to Computational Fluid Dynamics, the Finite Volume Method*, 2nd ed.; Pearson Education Limited: Harlow, UK, 2007; ISBN 978-0-13-127498-3.
34. Maliska, C.R. *Computational Heat Transfer and Fluid Mechanics*, 2nd ed.; LTC: Rio de Janeiro, Brazil, 2004. (In Portuguese)
35. Carslaw, H.S.; Jaeger, J.C. *Conduction of Heat in Solids*, 2nd ed.; Oxford University Press: New York, NY, USA, 1959; 510p.
36. Lima, A.G.B. Diffusion Phenomenon in Prolate Spheroidal Solids. A Case Study: Banana Drying. Ph.D. Thesis, State University of Campinas, Campinas, Brazil, 1999. Available online: <http://repositorio.unicamp.br/jspui/handle/REPOSIP/265133> (accessed on 24 October 2020). (In Portuguese)

37. Oliveira, V.A.B. Heat and Mass Transfer in the Interior of Solid with Prolate Spheroidal Shape Via Thermodynamic of Irreversible Processes. Ph.D. Thesis, Federal University of Campina Grande, Campina Grande, Brazil, 2006. Available online: <http://dspace.sti.ufcg.edu.br:8080/jspui/handle/riufcg/6853> (accessed on 24 October 2020). (In Portuguese)
38. Franco, C.M.R. Modeling, Simulation and Experimentation of the Continuous and Intermittent Drying of Elipsoidal Solids: Case Studies: Rough Rice Grain Drying. Ph.D. Thesis, Federal University of Campina Grande, Campina Grande, Brazil, 2016. Available online: <http://dspace.sti.ufcg.edu.br:8080/jspui/handle/riufcg/950> (accessed on 24 October 2020). (In Portuguese)

Publisher's Note: MDPI stays neutral with regard to jurisdictional claims in published maps and institutional affiliations.



© 2020 by the authors. Licensee MDPI, Basel, Switzerland. This article is an open access article distributed under the terms and conditions of the Creative Commons Attribution (CC BY) license (<http://creativecommons.org/licenses/by/4.0/>).